

Voidage Instabilities in Liquid Fluidized Beds

Eldin Wee Chuan Lim¹, Yee Sun Wong² and Chi-Hwa Wang^{1,2}

¹Department of Chemical and Biomolecular Engineering, National University of Singapore, 4 Engineering Drive 4, Singapore, 117576

²Singapore-MIT Alliance, 4 Engineering Drive 4, Singapore, 117576

Prepared for presentation at the 2005 AIChE Annual Meeting
Cincinnati, Ohio, October 30 - November 4, 2005.

Copyright © Eldin Wee Chuan, Yee Sun Wong, Chi-Hwa Wang
September, 2005

AIChE shall not be responsible for the statements or opinions contained in papers or printed in its publications

Introduction

Liquid fluidized beds in narrow tubes are well known to be susceptible to instabilities under certain operating conditions. One such instability is the appearance of one-dimensional voidage waves consisting of alternating regions of high and low particle concentrations along the bed. Several experimental studies on such phenomenon have been reported in the literature. Duru et al.¹ investigated experimentally this type of instability by measuring the shape of these voidage waves and relating them to solid phase viscosity and pressure functions of a continuum two-phase model. Duru and Guazzelli² observed the formation of bubbles in the same type of system resulting from the destabilization of such voidage wave structures and compared their experimental observations with previous analytical and numerical studies. Nicolas et al.³ also investigated the nature of such instabilities in liquid fluidized beds and suggested that the behavior of an unstable bed exhibiting voidage waves is determined by the external perturbations imposed and that the resulting instabilities are convective in nature.

Numerical Method

In the present study, the convective nature of voidage wave instabilities was investigated computationally using the Discrete Element Method (DEM) coupled with Computational Fluid Dynamics (CFD). The geometry of the fluidization system simulated consisted of a two-dimensional narrow channel of width 2 cm containing 2500 glass beads as the solids phase and water as the interstitial fluid. Each glass bead had a diameter of 1.0 mm and density 2500 kg m⁻³. The superficial velocities of the liquid used were 0.018 m s⁻¹ and 0.03 m s⁻¹. The base of the fluidization system was allowed to undergo simple harmonic motion when desired in order to facilitate the study of the effects of external perturbations on the stability of the bed. The amplitude and frequency applied when a vibrating base was simulated were 1.5 times the diameter of a glass bead (i.e. 1.5 mm) and 2 Hz respectively.

Following Cundall and Strack⁴, the equations in DEM governing the translational and rotational motions of individual solid particles are:

$$m_i \frac{dv_i}{dt} = \sum_{j=1}^N (f_{c,ij} + f_{d,ij}) + m_i g + f_{f,i} \quad (1)$$

$$I_i \frac{d\omega_i}{dt} = \sum_{j=1}^N T_{ij} \quad (2)$$

where m_i and v_i are the mass and velocity of particle i , N is the number of particles in contact with this particle, $f_{c,ij}$ and $f_{d,ij}$ are the contact and viscous contact damping forces respectively, $f_{f,i}$ is the fluid drag force due to an interstitial fluid, I_i is the moment of inertia of particle i , ω_i is its angular velocity and T_{ij} is the torque arising from contact forces which will cause the particle to rotate. The normal ($f_{cn,ij}$, $f_{dn,ij}$) and tangential ($f_{ct,ij}$, $f_{dt,ij}$) components of the contact and damping forces are calculated according to a linear force-displacement model:

$$f_{cn,ij} = -(\kappa_{n,i} \delta_{n,ij}) n_i \quad (3)$$

$$f_{ct,ij} = -(\kappa_{t,i} \delta_{t,ij}) t_i \quad (4)$$

$$f_{dn,ij} = -\eta_{n,i}(\mathbf{v}_r \cdot \mathbf{n}_i)\mathbf{n}_i \quad (5)$$

$$f_{dt,ij} = -\eta_{t,i}[(\mathbf{v}_r \cdot \mathbf{t}_i)\mathbf{t}_i + (\boldsymbol{\omega}_i \times \mathbf{R}_i - \boldsymbol{\omega}_j \times \mathbf{R}_j)] \quad (6)$$

where $\kappa_{n,i}$, $\delta_{n,ij}$, \mathbf{n}_i , $\eta_{n,i}$ and $\kappa_{t,i}$, $\delta_{t,ij}$, \mathbf{t}_i , $\eta_{t,i}$ are the spring constants, displacements between particles, unit vectors and viscous contact damping coefficients in the normal and tangential directions respectively, \mathbf{v}_r is the relative velocity between particles and \mathbf{R}_i and \mathbf{R}_j are the radii of particles i and j respectively. If $|f_{ct,ij}| > |f_{cn,ij}| \tan \phi + c$ then 'slippage' between the two contacting surfaces is simulated by a Coulomb-type friction law, $|f_{ct,ij}| = |f_{cn,ij}| \tan \phi + c$ where $\tan \phi$ is analogous to the coefficient of friction and c is a measure of cohesion between the two contacting surfaces.

The fluid drag force model due to Di Felice⁵ which is applicable over a wide range of particle Reynolds numbers was used for evaluating the fluid drag force. The equations in this model include:

$$f_{f,i} = f_{f0,i} \varepsilon_i^{-\chi} \quad (7)$$

$$f_{f0,i} = 0.5 c_{d0,i} \rho_f \pi R_i^2 |u_i - v_i| (u_i - v_i) \quad (8)$$

$$\chi = 3.7 - 0.65 \exp \left[-\frac{(1.5 - \log_{10} Re_{p,i})^2}{2} \right] \quad (9)$$

$$c_{d0,i} = \left(0.63 + \frac{4.8}{Re_{p,i}^{0.5}} \right)^2 \quad (10)$$

$$Re_{p,i} = \frac{2 \rho_f R_i |u_i - v_i|}{\mu_f} \quad (11)$$

where $f_{f0,i}$ is the fluid drag force on particle i in the absence of other particles, χ is an empirical parameter, ε_i is the local average porosity in the vicinity of particle i , $c_{d0,i}$ is the drag coefficient, $Re_{p,i}$ is the Reynolds number based on particle diameter, ρ_f is the fluid density, μ_f is the fluid viscosity and u_i is the fluid velocity.

The motion of the continuum gas phase is governed by the Navier-Stokes equations with interphase interactions taken into account as an additional source term in the momentum equation:

$$\frac{\partial \varepsilon}{\partial t} + \nabla \cdot (\varepsilon \mathbf{u}) = 0 \quad (12)$$

$$\frac{\partial (\rho_f \varepsilon \mathbf{u})}{\partial t} + \nabla \cdot (\rho_f \varepsilon \mathbf{u} \mathbf{u}) = -\varepsilon \nabla P + \nabla \cdot (\mu_f \varepsilon \nabla \mathbf{u}) + \rho_f \varepsilon \mathbf{g} - F \quad (13)$$

where \mathbf{u} is the velocity vector, ε is the local average porosity, P is the fluid pressure and F is the source term due to fluid-particle interaction.

Results and Discussion

Figure 1 shows 4 consecutive snapshots of the fluidized bed system obtained from the simulation. The time interval between each snapshot is 0.05 s and the dimensions are 16 cm (height) by 2 cm (width). Alternating bands of dense and dilute solid concentrations may be clearly discerned from the figure. There are approximately two dense and two dilute phases present in the

system under the present set of operating conditions. The coherent motion of these phases of the voidage wave up along the fluidized bed may also be observed. As such, the present simulation has been successful in reproducing the main qualitative feature of the phenomenon associated with voidage wave instability in a liquid fluidization system. It may also be stated that in the absence of a vibrating base, the fluidized bed was observed to expand slightly upon introduction of liquid with a superficial velocity and remain homogeneously fluidized with minimal tendency to develop such voidage wave instability (data not shown for brevity). This implied that the system was intrinsically stable in the absence of external perturbations while any internal noises were not sufficiently significant to cause instability. This was true for both liquid superficial velocities of 0.018 m s^{-1} and 0.030 m s^{-1} investigated in the initial phase of the present study. At the lower liquid superficial velocity of 0.018 m s^{-1} and in the presence of a vibrating base, a small amount of voidage waves could be observed in the system. These formed at the vibrating base but were propagated only a short distance up the bed. As the fluidized bed at this low superficial velocity was only expanded slightly and close to a packed condition, the likely reason for attenuation of the voidage waves could be the high effective solid viscosity. In contrast, when the liquid superficial velocity applied was 0.030 m s^{-1} such that the bed was expanded to a larger extent, voidage instabilities in the form of waves of high and low solid concentrations could be observed traveling up the expanded bed as shown in Figure 1. These clearly show the unstable nature of the system towards external perturbations and the convective characteristic of the resulting instability. In the following section, quantitative analyses of this phenomenon would be provided.

The instantaneous velocity vectors of particles illustrate the unique behavior of solid particles in a liquid fluidization system in the presence of voidage waves (data not shown). Particles switch periodically between generally upward and downward motions. These correspond to the passage of dense and dilute phases of the voidage wave through the particles respectively. In other words, when a dense phase of the wave propagates through a section of the bed, particles in that section were observed to be moving in the upward direction and vice versa. For the present case studied, the frequency and amplitude of the vibrating base were 2 Hz and 1.5 mm respectively. The characteristic frequency of the periodic motion of the solid particles was also observed to be about 2 Hz. The characteristic length scale of the size of a dense (or dilute) region of the voidage wave is about 1.0 – 1.5 cm.

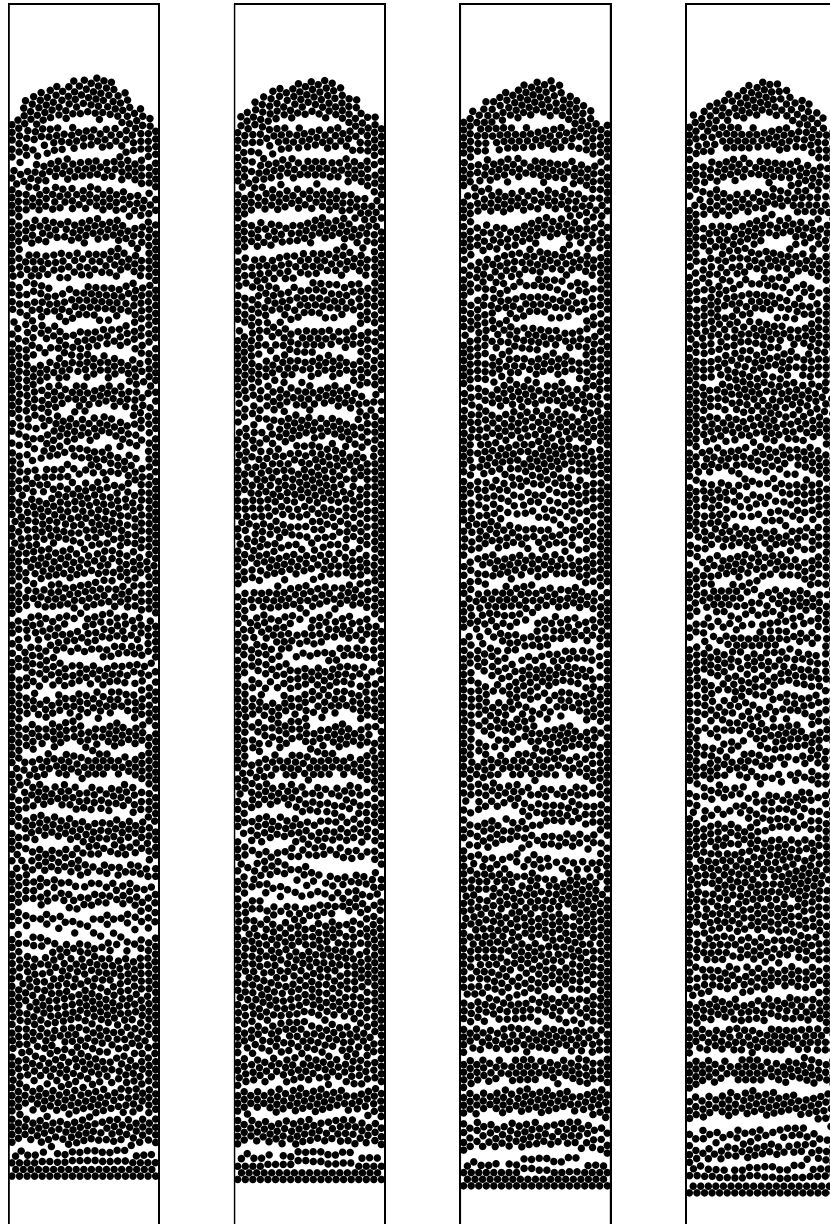


Figure 1 Voidage waves in a liquid fluidized bed operating at the following conditions: Liquid superficial velocity at inlet of 0.03 m s^{-1} , vibrating amplitude and frequency of base of 1.5 mm and 2 Hz respectively. Time interval between each frame shown is 0.05 s . Dimensions of the system are 16 cm (height) by 2 cm (width).

Figures 2a, b show the power spectral of solid fraction obtained at positions 1 cm and 10 cm above the vibrating base respectively. These were obtained by fast Fourier Transforms of the corresponding solid fraction signals with respect to time. It may be seen that the characteristic frequency of the voidage wave is also equal to that of the vibrating base. In addition, there may be higher or lower harmonics in the vicinity of this characteristic frequency (in the range 1 – 5 Hz) as shown in Figure 2a. However, only the driving frequency of 2 Hz of the base has been manifested as the characteristic frequency of the voidage wave up to a height of 10 cm along the fluidized bed. The various other harmonics are propagated a smaller distance. Figure 2b shows that other than the frequency which is exactly twice (4 Hz) that of the characteristic frequency, these are no longer present in the solid fraction signal at 10 cm from the vibrating base.

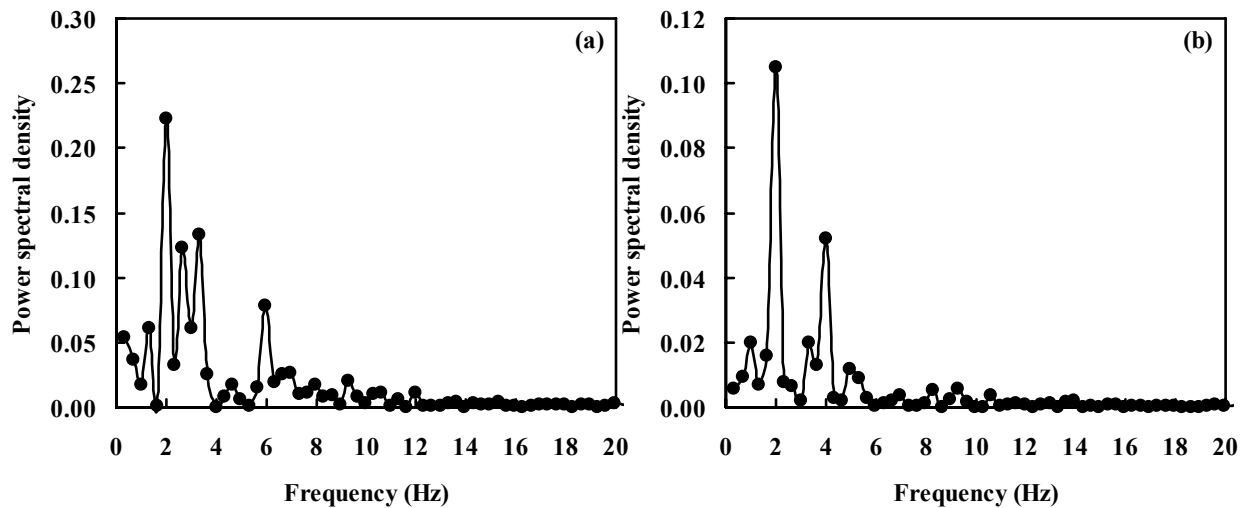


Figure 2 Power spectrum of solid fraction profile obtained at (a) 1 cm, (b) 10 cm above the vibrating base.

A comparison of the granular temperature profiles of the liquid fluidized bed operating in both the stable and unstable modes provided useful insights to the mechanistic nature and origin of such voidage instabilities. The stable bed exhibited almost negligible granular temperatures at all positions along the height of the bed (data not shown) while its unstable counterpart exhibited noisy but generally sinusoidal granular temperature profiles (Figure 3a). These corresponded to the presence of low and high Reynolds stresses in the system respectively and seemed to suggest possible correlations between such stresses and the onset of instability. This observation is consistent with the conclusion made by Ham *et al.*⁶ whose flow visualization experiments and detailed quantitative measurements showed Reynolds stresses due to particle velocity fluctuations to be the main contributor to the formation of voidage instabilities. Furthermore, the power spectrum of the granular temperature obtained from the present simulation also shows that its characteristic frequency matches that of the vibrating base and solid fraction (Figure 3b).

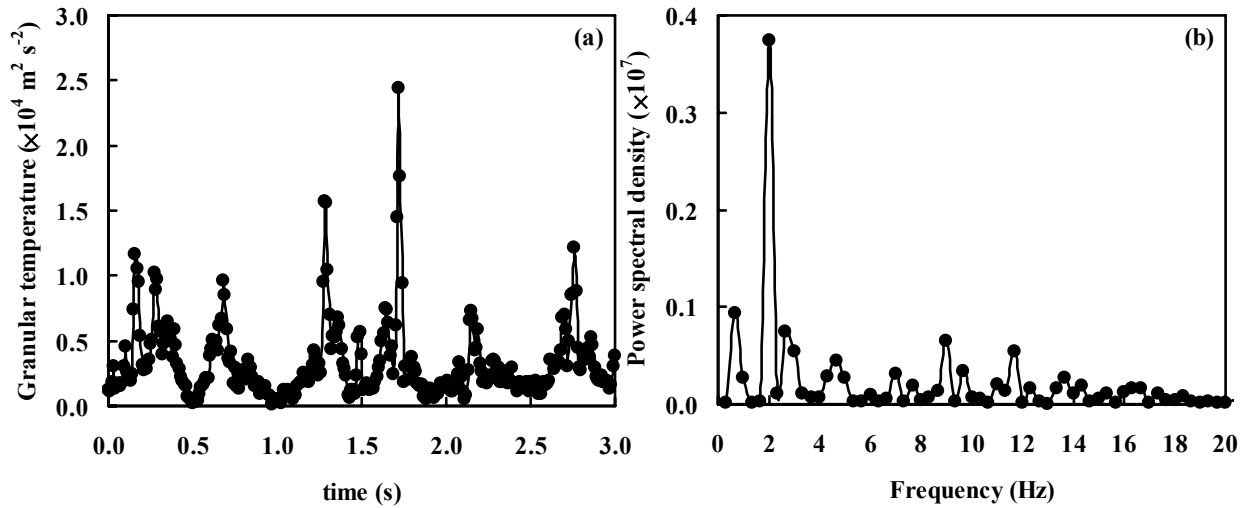


Figure 3 (a) Variation of spatially averaged granular temperature of solids 5 cm above the vibrating base with respect to time, (b) Power spectrum of the granular temperature profile from (a).

Despite the convective nature of the voidage waves which originate at the vibrating base and travel up along the length of the fluidized bed, one interesting feature of such instabilities observed in the present simulations is the highly localized motion of individual particles. As discussed earlier, solid particles move upwards when a dense phase of the voidage wave passes through and settle downwards in the dilute phase of the wave. However, the overall motion of each individual particle was observed to be highly restricted to a small region within the system. Taking a Lagrangian point of view, the positions of four arbitrarily selected particles were tracked for a period of 6 s corresponding to 12 cycles of the vibrating base. Figure 4a shows the position of each particle at 1 s intervals. Regardless of the precise starting location of the particle within the system, it may be seen that there is very restricted motion in both the axial (vertical) and lateral (horizontal) directions. Each particle seems to be ‘trapped’ within a small cell whose dimensions are similar to that of a dense or dilute phase of the voidage wave. However, when the base is vibrated at a frequency of 1 Hz, with all other operating parameters unchanged, the size of the cell in which each particle is trapped remains substantially similar (Figure 4b). The extent of motion of individual particles does not seem to be significantly affected by the frequency of the vibrating base. On the other hand, it may be observed from Figure 5 that the macroscopic structure of the voidage wave has been changed with the reduction in vibrating frequency. Both the solid distribution in the fluidized bed and the velocity vectors of the particles shown in the figure suggest that there is only half a voidage wave containing one dense and one dilute phase present. In other words, the effective wavelength of the voidage wave has been doubled with a reduction of vibrating frequency of the base to half its original value.

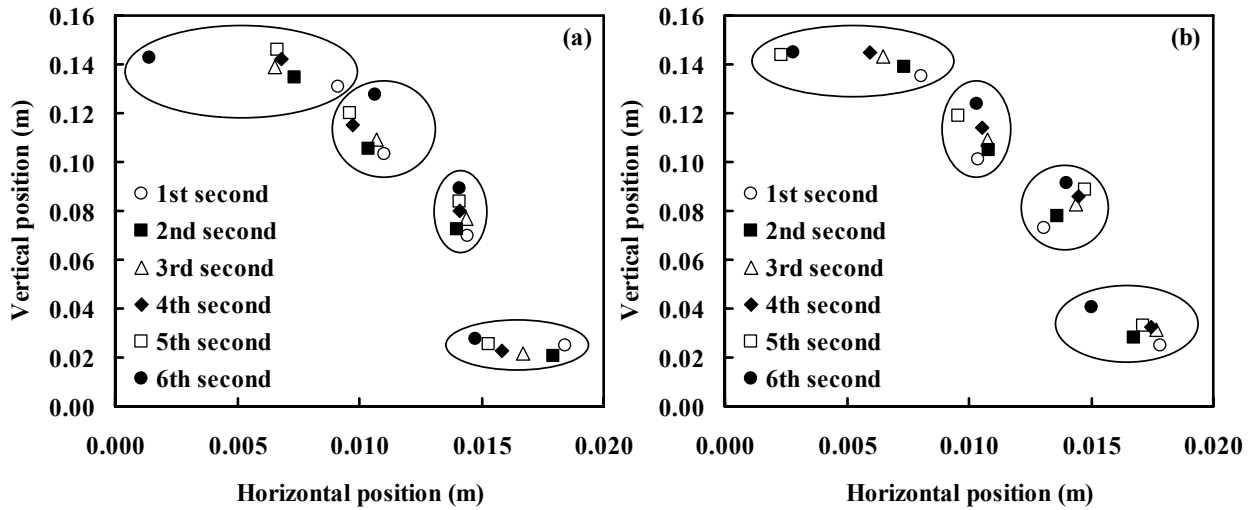


Figure 4 Positions of four arbitrarily selected particles at 1 s intervals. Vibrating frequency of the base applied is (a) 2 Hz, (b) 1 Hz.

Conclusions

The computer simulations combining the Discrete Element Method with Computational Fluid Dynamics calculations performed in this study have reproduced the phenomenon of voidage wave formation in a liquid fluidized bed system subjected to external perturbations. A uniform inlet velocity was applied and the base of the system was allowed to undergo simple harmonic motions to simulate the introduction of small external disturbances. Voidage waves consisting of alternating regions of high and low solid concentrations were observed to form and travel in a coherent manner along the fluidized bed. Solid particles were seen to move upwards when a dense phase of the wave passed through their positions and settle downwards otherwise. The characteristic frequency of such oscillatory motions of solid particles was obtained by a fast Fourier Transform of the vertical component of solid velocities and observed to match the vibrating frequency of the base. Similarly, the characteristic frequencies of solid fraction and granular temperature which also exhibited periodic variations with respect to time were found to be equal to the vibrating frequency of the base. The voidage waves formed as a result of instability in such liquid fluidized bed systems are traveling waves with dense and dilute phases being convected along the bed. The effective wavelength of such waves in terms of the distance between two adjacent dense or dilute phases was found to depend substantially on the frequency of vibration of the base. However, the motion of individual particles was observed to be highly restricted to a small region or cell whose dimensions did not seem to depend significantly on the vibrating frequency. Despite the convective nature of such waves, the phenomenon is a highly localized one at the individual particle level. This may have important implications for the operations of such liquid fluidization system such as with regards to the effectiveness with which solids mixing can be accomplished in such systems and others.

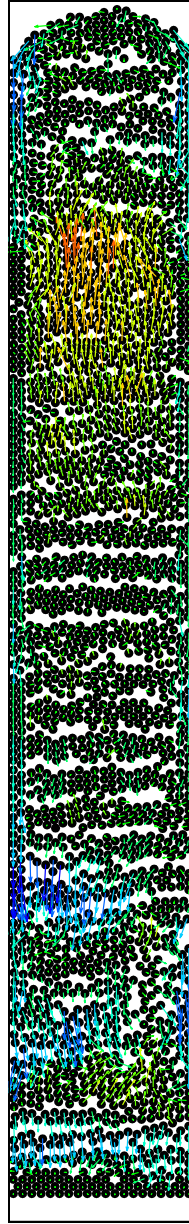


Figure 5 Voidage wave formed at a vibrating frequency of 1 Hz. Other operating parameters are as for Fig. 1.

Literature Cited

1. Duru, P., M. Nicolas, J. Hinch, E. Guazzelli. Constitutive laws in liquid-fluidized beds. *Journal of Fluid Mechanics*, 452, 371–404. 2002.
2. Duru, P. and E. Guazzelli. Experimental investigation on the secondary instability of liquid-fluidized beds and the formation of bubbles. *Journal of Fluid Mechanics*, 470, 359–382. 2002.
3. Nicolas, M., J.-M. Chomaz, D. Vallet, E. Guazzelli, E. Experimental investigations on the nature of the first wavy instability in liquid fluidized beds. *Physics of Fluids*, 8, 1987–1989. 1996.

4. Cundall, P. A. and O. D. L. Strack. A discrete numerical model for granular assemblies. *Geotechnique*, 29, 47–65. 1979.
5. Di Felice, R. The voidage function for fluid-particle interaction systems. *Int. Journal Multiphase Flow*, 20, 153–159. 1994.
6. Ham, J. M., S. Thomas, E. Guazzelli, G. M. Homsy, M.-C. Anselmet. An experimental study of the instability of liquid-fluidized beds. *International Journal of Multiphase Flow*, 16, 171–185. 1990.